Multiple Faults Detection in PMSM Drives Using MultiResolution Analysis

Saïda Ben Slimen
LR11ES15 LSE
Université de Tunis El Manar, ENIT
1002, Tunis, Tunisie
benslimene.saida@gmail.com

Manef Bourogaoui
LR11ES15 LSE
Université de Tunis El Manar, ENIT
1002, Tunis, Tunisie
Université de Gafsa, ENIGA
2100, Gafsa, Tunisie
manef_bourogaoui_lse@yahoo.fr

Houda Ben Attia Sethom
LR11ES15 LSE
Université de Tunis El Manar, ENIT
1002, Tunis, Tunisie
Université de Carthage,
ENICarthage 2035, Tunis, Tunisie
houda.benattia@enicarthage.rnu.tn

Abstract -- **This paper deals with multiple faults detection in Permanent Magnet Synchronous Motor (PMSM) based Adjustable Speed Drives (ASD) using a signal processing technique. Indeed, in this study, the Discrete Wavelet Transform (DWT) based–Multiresolution Analysis (MRA) algorithm is used as a detection technique in order to generate a unique signature for each studied fault. The considered faults are: a total loss of the current sensor information, a total loss of the position sensor information, a single open motor phase, a single IGBT open-circuit, two IGBTs open-circuit in two different inverter legs. Simulation results were carried out under MATLAB-Simpower ® environment, in order to conclude to the relevance and effectiveness of the proposed technique in faults detection**
Index Terms—**PMSM, ASD, fault, detection, DWT-MRA.**

I. INTRODUCTION

Thanks to their advantages such as high efficiency, high speed operation, reliability, robustness and compactness, the Permanent Magnet Synchronous Motors (PMSMs) based Adjustable Speed Drives (ASD) are suitable candidates for several applications such as aerospace, military, medical, robotic and land transports, [1-3].

However, mechanical and electrical faults may affect the PMSM ASD leading to very dangerous operating conditions. Giving this fact, accurate and fast detection of these faults should be performed to avoid the system breakdown and to reduce its down time in order to keep the PMSM ASD performances and to ensure the system service continuity [1], [4-12].Therefore, it is paramount to detect abrupt faults as early as possible.

In fact, several techniques have conducted to efficient fault detection in the PMSM drives. Nevertheless, in the literature, researchers have not worked on the effectiveness of a given method to detect multiple faults that may occur on a drive. In the majority of the studied cases, a detection method is efficient for one fault and not for another [4], [6], [11-12].

In this paper, the considered method is the Discrete Wavelet Transform-based MultiResolution Analysis (DWT–MRA). It consists in a strong signal processing technique that has proved its capability to detect abrupt changes caused by faults occurrence in PMSM ASDs. In our previous works, the use of this technique, based on real stator currents, as a fault detection tool for position sensor breakdown in a PMSM ASD, gave acceptable results, [8-10].

In this paper, the novel contribution consists in the normalized stator currents analysis through the DWT–MRA technique in order to generate a signature for each considered fault. Thus, the challenge is then to highlight the effectiveness of this method for multiple faults detection in the considered PMSM drive. These faults are: a total loss of the current sensor information, a total loss of the position sensor information, a single open motor phase, a single IGBT open-circuit, two IGBTs open-circuit in two different inverter legs.

The sections of this paper are summarized as follows.

First, the PMSM drive operating under each fault occurrence conditions is analyzed. Second, the DWT-MRA is used as a detection technique of the studied faults based on the normalized stator currents. Third, a discussion is carried out to highlight the effectiveness of the used technique for the PMSM drive multiple faults detection.

II. PMSM DRIVE OPERATING UNDER FAULTY CONDITIONS

A. PMSM drive model

The studied system includes a PMSM, a PWM voltage inverter, current and position sensors. A closed loop flux vector control strategy is considered in order to achieve high PMSM drive performances, Fig.1.

The PMSM model has been developed in the (d, q) reference frame. Its mathematical model is described by equations (1-5). The PMSM parameters are listed in the table II of the appendix. The stator voltages are described by equations (1) and (2).

$$v_{sd} = R_s i_{sd} + l_{sd}\frac{di_{sd}}{dt} - \dot{\theta}_e l_{sq} i_{sq} \qquad (1)$$

$$v_{sq} = R_s i_{sq} + l_{sq}\frac{di_{sq}}{dt} + \dot{\theta}_e l_{sd} i_{sd} + \dot{\theta}_e \Psi_{PM} \qquad (2)$$

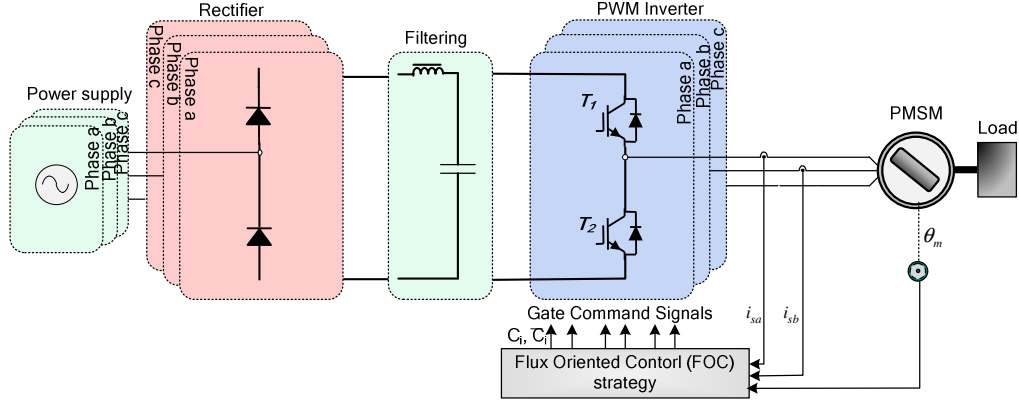where v_{sd}, v_{sq}, i_{sd} and $i_{sq}$are the direct and quadrature stator voltages and currents.

Fig. 1. The PMSM drive and its Flux Oriented Control scheme.

The electromagnetic torque is given by equation (3).

$$C_{em} = \frac{3}{2} p((l_{sd} - l_{sq})i_{sd}i_{sq}) + \Psi_{PM} i_{sq} \qquad (3)$$

The mechanical equation is given by (4).

$$\frac{J}{p}\frac{dw_e}{dt} = C_{em} - C_r - f_v \frac{w_e}{p} \qquad (4)$$

where:

$$\frac{d\theta_e}{dt} = w_e \qquad (5)$$

The Park vector components i_{sd} and i_{sq} resulting from the stator currents i_{sabc} Park transformation are given by (6) and (7), respectively.

$$i_{sd} = \frac{2}{3}\left(\cos(\theta_e)i_{sa} + \cos(\theta_e - \frac{2\pi}{3})i_{sb} + \cos(\theta_e + \frac{2\pi}{3})i_{sc}\right) \qquad (6)$$

$$i_{sq} = \frac{2}{3}\left(-\sin(\theta_e)i_{sa} - \sin(\theta_e - \frac{2\pi}{3})i_{sb} - \sin(\theta_e + \frac{2\pi}{3})i_{sc}\right) \qquad (7)$$

Simulation results were carried out under MATLAB-Simpower®, for the following operating conditions: The rotor speed reference is set at 600 rpm with a load torque equal to 10% of C_r.

In the following subsections, the PMSM ASD model under study will be used in order to well analysing the impact of different faults on the PMSM behavior, namely a total loss of the current sensor information, a total loss of the position sensor information, a single open motor phase, a single IGBT open-circuit, two IGBTs open-circuit in two different inverter legs. The study particularly focuses on the impact of each fault occurrence on the stator currents. In order to compare the impacts of the faults on the PMSM drive behavior, all faults have been applied at the same instant t_f=0.75s.

B. *Current sensor total loss information fault*

In this study, two current sensors are used in normal operation, but when a current sensor fail, an important degradation in the closed loop control strategy can be observed. The failure may be caused by the sensor breakdown which is the case of the studied fault [7]. So it is critical to detect the fault as rapid as possible.
Fig. 2 depicts a sudden change in the balanced stator currents i_{sabc} after a total loss of the *a*-phase current sensor information. This change is translated by the vanish of

the measured stator current i_{sa} and the disturbance of the other measured stator currents i_{sb} and i_{sc}.

C. *Position sensor total loss information fault*

The position sensor is used for measuring position/speed, which is the paramount controlled variable for closed loop operation. Thus, its erroneous values lead to the instability of the PMSM ASD. This fault may be caused by a breakdown of the sensor, of its supply or of its connexions as well as the current sensor, which are the common possible faults for sensors [8-10].
Fig. 3 shows the stator currents i_{sabc} before, during and after a total loss of the position sensor information fault occurrence. It can be well noted that the fault introduces a DC component into the stator currents. Then, the PMSM is badly supplied, and it is not able to operate in closed loop conditions.

D. *Single phase open circuit fault*

This type of fault may be caused by a mechanical failure of the machine terminal connector, an internal winding rupture, or by an electrical failure in one of the inverter phase legs, which it is the case of this study [11-12].
Fig. 4 shows the three phase stator currents before, during and after a single phase open circuit fault occurrence. As a consequence, the stator current i_{sa} becomes null and, as for the current sensor fault case, the other measured stator currents i_{sb} and i_{sc} are disturbed.

E. *Single IGBT open-circuit fault*

This fault may be the consequence of a failure in the IGBT electronic components or in its control circuit [4], [5]. When an open IGBT fault occurs in the inverter and the closed loop control strategy remains unchanged, the PMSM can be able to continue working in some cases, but the system stability cannot be guaranteed. For that, it is necessary to detect rapidly the fault occurrence.
Fig. 5 shows the impact of the IGBT open-circuit fault on the stator phase currents. As the faulty IGBT is chosen to be *T1*, then, the stator current i_{sa} becomes null for the positive half period. On the other hand, the stator currents i_{sb} and i_{sc} contain a DC component and become in phase opposition in order to compensate the loss of the defective phase current.

F. Two IGBTs open-circuit in two different inverter legs

This subsection deals with the case of two IGBTs open circuit fault in two different legs. It should be noted that when this fault occurs in the power converter, the PMSM will be badly controlled and may lead to the PMSM ASD performances degradation. Therefore, it is critical to detect the fault occurrence rapidly in order to ensure the system stability and its service continuity.
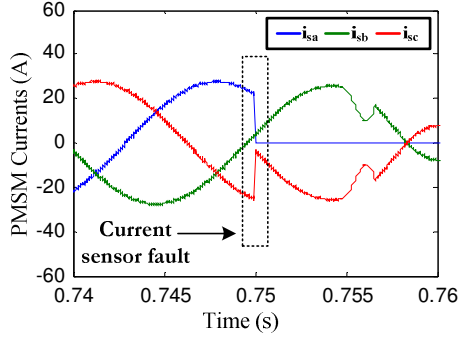
Fig. 6 shows the impact of a simultaneous open-circuit fault of the two IGBTs T_1 and T_4 on the stator currents i_{sa}, i_{sb} and i_{sc}. Indeed, the stator currents i_{sa} and i_{sb} become null for the positive half period. Consequently, the three stator currents become highly unbalanced and this may lead to dangerous consequences on the drive operating, [4].
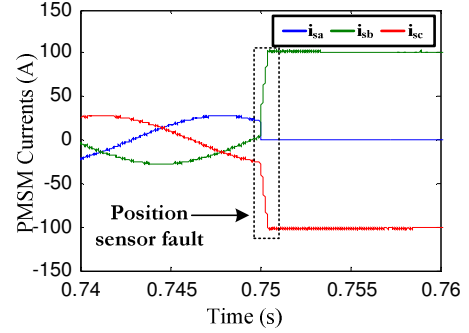

Fig. 2. The impact of the current sensor breakdown on the stator currents i_{sa}, i_{sb} and i_{sc}, under 10% load torque and 600 rpm operating conditions.

Fig. 3. The impact of a position sensor breakdown on stator currents i_{sa}, i_{sb} and i_{sc} under 10% rated load torque and 600 rpm operating conditions.
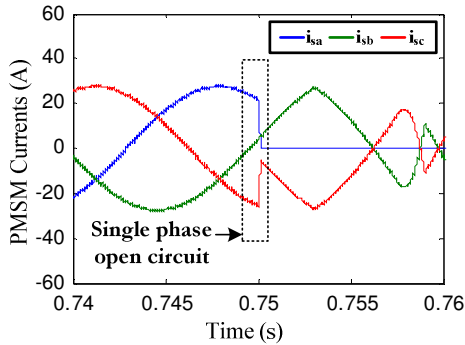

Fig. 4. The impact of a single phase open circuit on the stator currents i_{sa}, i_{sb} and i_{sc} under 10% rated load torque and 600 rpm operating conditions.
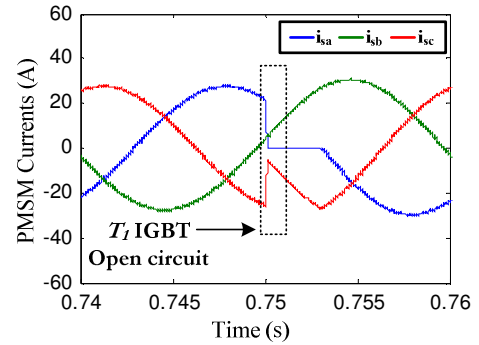

Fig. 5. The impact of the T_1 IGBT open-circuit on the stator currents i_{sa}, i_{sb} and i_{sc} under 10% rated load torque and 600 rpm operating conditions.
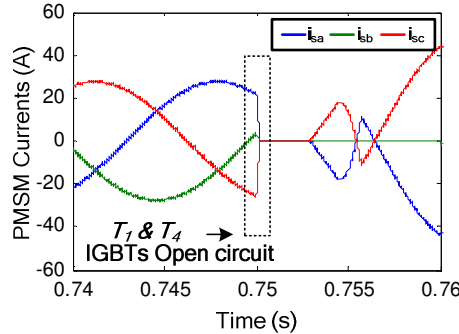

Fig. 6. The impact of T_1 and T_4 IGBTs open-circuit in inverter legs 1 and 2 on the stator currents i_{sa}, i_{sb} and i_{sc} under 10% rated load torque and 600 rpm operating conditions.

III.   DWT-MRA BASED MULTIPLE FAULTS DETECTION

A. Application of the MRA to the normalized PMSM currents signals

As it has been mentioned above, this study aims to ensure an early, rapid and effective multiple faults detection by defining a signature for each considered fault independently of operating conditions.

This aim will be reached using the Discrete Wavelet Transform-based MultiResolution Analysis (DWT–MRA)

technique in a novel way. Indeed, the originality of the proposed technique consists in applying the MRA to the normalized stator currents i_{sa-n} and i_{sb-n}.

In fact, these currents were normalized by the instantaneous module of (d, q) currents.

The normalized stator currents are calculated as follows:

$$i_{sa,b-n} = \frac{i_{sa,b}}{i_s} \tag{8}$$

where the instantaneous module i_s is given by the equation (9).

$$i_s = \sqrt{\left(i_{sd}^2 + i_{sq}^2 \right)} \tag{9}$$

B. DWT-MRA technique

In recent years wavelet analysis technique has been applied to many areas of signal processing [5], [8-10]. For this section, the DWT–MRA technique is recalled. Indeed, the DWT–MRA theory is based on a numerical filter bank, which is composed by low-pass filters (LPF) and high-pass filters (HPF), these filters are used for the construction of the MultiRésolution time-frequency plane.

The MRA analyzes a numerical signal $S(n)$ through many frequency bands with different resolutions by decomposing it into approximations and details signals information [14].

The approximation and detail signals, which are the outputs of the low-pass and high-pass filters respectively, are given by equations (10) and (11).

$$a_i(n) = \sum_{k=0}^{N-1} s(k) h(n-k) \qquad (10)$$

$$d_i(n) = \sum_{k=0}^{N-1} s(k) g(n-k) \qquad (11)$$

The decomposition of signals into frequency sub-bands is limited by the maximum level J, given by equation (12).

$$2^{J\,\max} \le N \qquad (12)$$

where N is the number of samples, whose value is equal to 10^6 in this study case.

Consequently, the maximum decomposition level J is chosen equal to 7. This level is considered sufficient for effective faults detection. Thus, the used mother wavelet is the 2nd order Daubechies *DB2*.Indeed, the use of this mother wavelet allows highlighting in the best way the fault occurrence transients.

C. Multiple Faults Detection using DWT-MRA

In this subsection, simulation results are given based on the DWT-MRA technique for all the studied faults. As it was mentioned above, the analysis was performed based on both normalized stator currents i_{sa-n} and i_{sb-n} in order to generate more information about faults signatures.

Indeed, Fig. 7, 8, 9, 10 and 11 present the high and low frequency details signals obtained from the DWT–MRA analysis of the normalized stator currents i_{sa-n} and i_{sb-n} regarding the current sensor, the position sensor, the single phase open circuit, the single IGBT open circuit and the two IGBTs open-circuit faults, respectively. It is mandatory to note that, for a better illustration of the obtained results, only the details signals that highlight abrupt changes caused by the considered faults occurrences have been presented in this paper.

It can be concluded that, significant abrupt changes in high frequency details signals contents appear for all the considered faults. Thus, thanks to the characteristics of the normalized stator currents, a threshold can be fixed for the high frequency detail signal independently of the PMSM operating conditions.

As a consequence and under different PMSM ASD faulty conditions, the generation of fault signatures can be ensured from both i_{sa-n} and i_{sb-n} details signals.

Therefore, comparisons between details signals are performed and presented in the coming section in order to generate signature for each fault occurrence.

It should be noted that the aim of this paper is the detection of multiple faults as early as possible. For that reason, a well-developed and detailed study must be carried out in order to guarantee a relevant detection based on details signals, which allow treating information about fault occurrence or false alarm cases.

IV. DISCUSSIONS

Regarding the obtained results, a comparative study was carried out in order to highlight the effectiveness and the relevance of the used detection technique to distinguish the studied faults.Indeed, the detection is based on the abrupt changes characteristics analysis in the normalized stator currents and the definition of fixed thresholds for details signals.

According to Fig. 7, 8, 9, 10 and 11, the detection of all studied faults is possible using the DWT–MRA technique since changes due to faults occurrence appear in details signals. Indeed, table I summarizes the details and the fixed thresholds that can be considered for each fault detection. In this step, the question is how to distinguish between these faults.

In fact, a classification can be deduced. There are two sets of faults. The first set includes the current sensor fault and the T_1 and T_4 IGBTs open-circuit fault since their effect appear in all details signals d_{1-7} according to Fig. 7 and 11, respectively. Whereas, the second set includes the other faults, namely the position sensor, the T_1 IGBT open circuit and the single open phase faults. However, for the two sets, it is difficult to identify the faulty component.

Giving this fact, the DWT–MRA itself is not sufficient for faults localization. Therefore, it is important to address other methods in order to ensure an efficient fault localization.
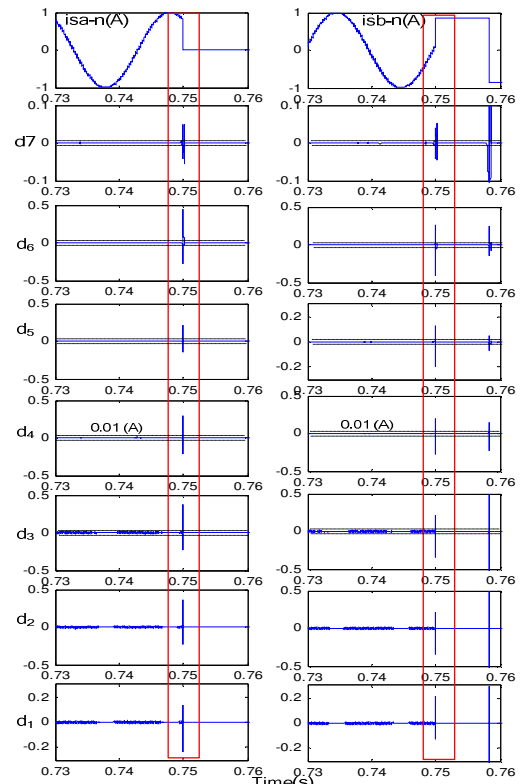

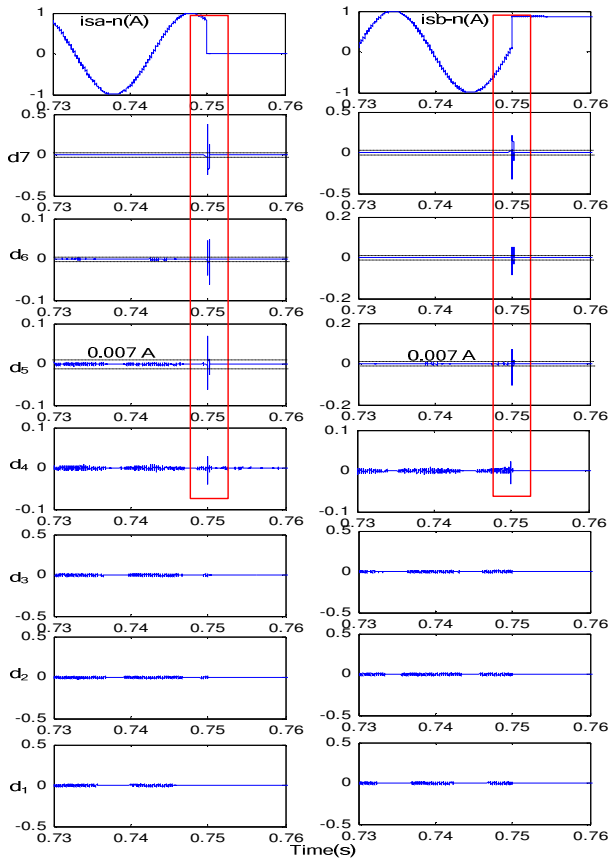Fig. 7. Current sensor fault detection using stator currents i_{sa-n} and i_{sb-n} MRA

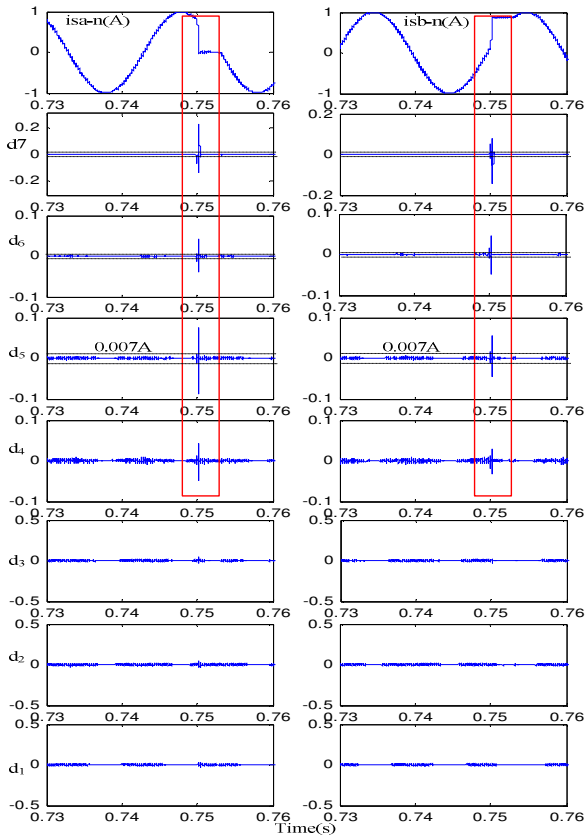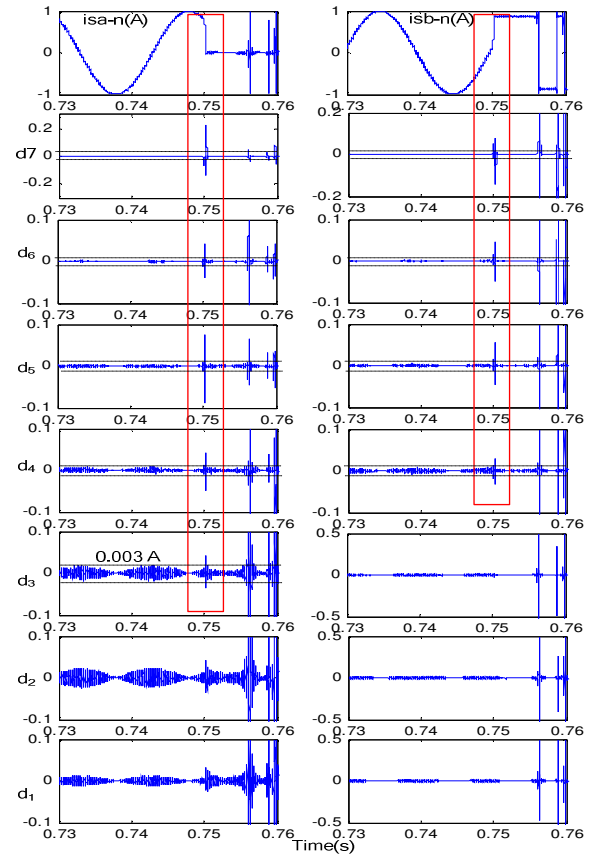Fig. 8. Position sensor fault detection using stator currents i_{sa-n} and i_{sb-n} MRA

Fig. 9. Single open phase fault detection using stator currents i_{sa-n} and i_{sb-n} MRA
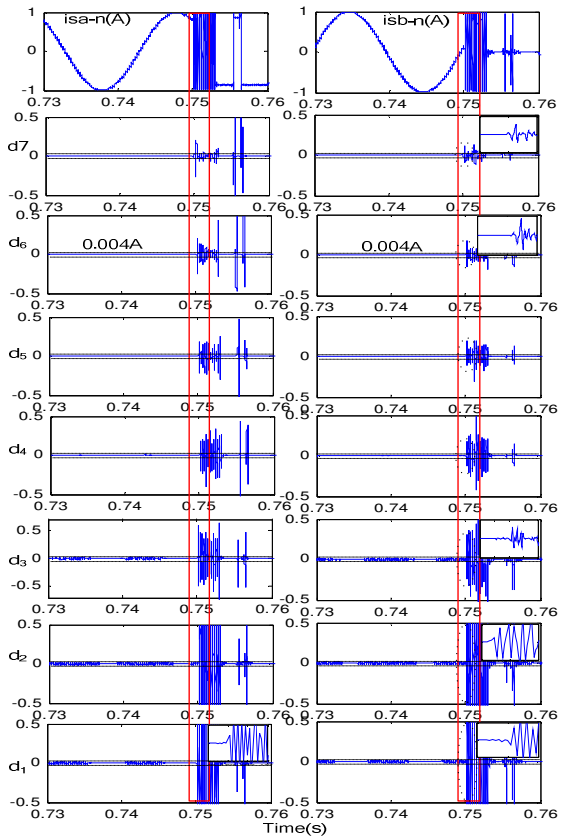

Fig. 10. T_1 IGBT open circuit fault detection using stator currents i_{sa-n} and i_{sb-n} MRA

Fig. 11. T_1 and T_4 IGBTs open circuit fault detection using stator currents i_{sa-n} and i_{sb-n} MRA

TABLE I
THE CONSIDERED THRESHOLDS FOR FAULTS DETECTION

Thresholds (10⁻²)	Details signals													
	$i_{sa\text{-}n}$							$i_{sb\text{-}n}$						
	d_1	d_2	d_3	d_4	d_5	d_6	d_7	d_1	d_2	d_3	d_4	d_5	d_6	d_7
Current sensor	2	3	3	2	0.7	0.4	0.3	2	3	3	2	0.7	0.4	0.3
T_1&T_4 IGBTs open circuit	2	3	3	2	0.7	0.4	0.3	2	3	3	2	0.7	0.4	0.3
T_1 IGBT open circuit	▨	▨	▨	2	0.7	0.4	0.3	▨	▨	▨	2	0.7	0.4	0.3
Position sensor	▨	▨	▨	2	0.7	0.4	0.3	▨	▨	▨	2	0.7	0.4	0.3
T_1 IGBT open circuit	▨	▨	▨	2	0.7	0.4	0.3	▨	▨	▨	2	0.7	0.4	0.3
Single phase open circuit	▨	▨	3	2	0.7	0.4	0.3	▨	▨	▨	2	0.7	0.4	0.3

	Possible fault detection
▨	*Not possible fault detection*

V. CONCLUSION

In this paper, a multiple faults detection has been presented for PMSM ASDs. These faults are: a total loss of the current sensor information, a total loss of the position sensor information, a single phase open-circuit, a single IGBT open-circuit, two IGBTs open-circuit in two different inverter legs. The detection technique has been based on the MultiResolution Analysis. It requires only the normalized measured currents of the *a* and *b* PMSM phases.

Simulation results of the PMSM drive operating under multiple faults conditions were presented and discussed according to the signals details that were useful for the detection based on the normalized stator currents in order to define fixed thresholds. This consists in a first step before dealing with the fault localization, which can be ensured by using other methods to reach the objective of generating a signature for each fault affecting the PMSM drive.

VI. APPENDIX

TABLE. II
PMSM PARAMETERS

Variable	Notation	Value
Rated power	P	53 kW
Rated current	I_n	122 A
DC bus voltage	V_{DC}	560 V
Maximal current	I_{max}	368 A
Rated torque	C_n	832 Nm
Rated flux	Ψ_{PM}	0.5 Wb
Rated speed	N_n	600 rpm
Armature resistance	R_s	0.087 Ω
Poles pairs number	p	5

TABLE. III
FREQUENCY BANDS DECOMPOSITION

Decomposition level	Frequency bands (Hz)	
	a_i	d_i
7	0 – 7812.5	7812.5– 15625
6	0 – 15625	15625– 31250
5	0 – 31250	31250 – 62500
4	0 – 62500	62500 – 125000
3	0 – 125000	125000 – 250000
2	0 – 250000	250000 – 500000
1	0 – 500000	500000 – 1000000

VIII. REFERENCES

[1] P. Rodriguez, S. Sahoo, C. T. Pinto, and M. Sulowicz, "Field Current Signature Analysis for Fault Detection in Synchronous Motors," IEEE 10th International Symposium on diagnostics for Electrical Machines, Power Electronics and Drives (SDEMPED), pp. 246-252, Sept. 2015.

[2] C. Zoeller, M. A. Vogelsberger, R. Fasching, and W. Grubelnik, "Evaluation and Current-Response Based Identification of Insulation Degradation for High Utilized Electrical Machines in Railway Application," IEEE 10th International Symposium on Diagnostics for Electrical Machines, Power Electronics and Drives (SDEMPED), pp. 266-272, Sept. 2015.

[3] Q. T. An, L. Sun, and L. Z. Sun, "Current Residual Vector Based Open-Switch Fault Diagnosis of Inverters in PMSM Drive Systems," IEEE Trans. On Power Electron, vol. 30, pp. 2814-2827, May. 2015.

[4] J. O. Estima, and A. J. M. Cardoso, "A New Approach for Real-Time Multiple Open-Circuit Fault Diagnosis in Voltage Source Inverters," IEEE Trans. On Ind Appl, vol. 47, pp. 2487-2494, Nov. 2011.

[5] H. Ben Attia Sethom, and M. Ajjabi Ghedamsi, "Intermittent Misfiring Default a PWM Inverter Using Wavelet Decomposition," Journal of Electrical Systems, pp. 222-234, 2008.

[6] S. Diao, Z. Makni, J. F. Bisson, D. Diallo, and C. Marchand, "Current Sensor Fault Diagnosis in the Stationary Frame for PMSM Drive in Automotive Systems," IEEE International conference on Ecological Vehicles and Renewable Energies (EVER), pp. 1-7, March. 2014.

[7] I. Jlassi, S. Khojet El Khil, and N. Mrabet Bellaaj, "Power Switch and Current Sensor Fault-Tolerant Control of PMSG Drives for Wind Turbine Systems," IEEE 10th International Symposium on Diagnostics for Electrical Machines, Power Electronics and Drives (SDEMPED), pp. 401-407, Sept. 2015.

[8] M. Bourogaoui, H. Berriri, H. Ben Attia Sethom, and I. Slama. Belkhodja, "Encoder Disturbance Fault Detection in PMSM Drives," Journal of Electrical Systems, vol. 10, no. 2, pp. 194–208, June. 2014.

[9] M. Bourogaoui, I. Jlassi, S. Khojet El Khil, and H. Ben Attia Sethom, "An Effective Encoder Fault Detection in PMSM Drives at Different Speed Ranges," IEEE, 10th International Symposium on Diagnostics for Electrical Machines, Power Electronics and Drives (SDEMPED), pp. 90-96, Sept. 2015.

[10] M. Bourogaoui, H. Ben AttiaSethom, and I. Slama Belkhodja, "Real-time Encoder Faults Detection and Rotor Position Estimation for Permanent Magnet Synchronous Motor Drives Fault Tolerant Sensorless Control using Digital Signal Controller," Journal of Mathematics and Computers in Simulation, Elsevier, Oct. 2015.

[11] B. A. Welchko, T. M. Jahns, and S. Hiti, "IPM Synchronous Machine Drive Response to a Single Phase Open Circuit Fault," IEEE Trans. on Power Electron, vol. 17, pp. 764-771, no. 5, Sept. 2002.

[12] A. Khlaief, M. Boussak, and M. Gossa, "Open Phase Faults Detection in PMSM Drives Based on Current Signature Analysis," IEEE in International Conference on Electrical Machines (ICEM), pp. 1-6, Sept. 2010.

[13] L. A. Kozionov, M. Kalinkin, A. Natekin, and A. Loginov, "Wavelet-Based Sensor Validation: Differentiating Abrupt Sensor Faults from System Dynamics," IEEE 7th International Symposium on Intelligent Signal Processing (WISP), pp. 1-5, Sept. 2011.

[14] S. Mallat, "A Theory for Multiresolution Signal Decomposition: The Wavelet Representation," IEEE Trans. Pattern Anal. Mach. Intell, vol. 11, no. 7, pp. 674-693, 1989.